Chemiluminescence excited paper-based photoelectrochemical competitive immunosensing based on porous ZnO spheres and CdS nanorods

Guoqiang Sun [a], Yan Zhang [a], Qingkun Kong [a], Chao Ma [a], Jinghua Yu [a], Shenguang Ge [b], Mei Yan *[a] and Xianrang Song [c]

[a] *Key Laboratory of Chemical Sensing & Analysis in Universities of Shandong, School of Chemistry and Chemical Engineering, University of Jinan, Jinan 250022, P. R. China.*

[b] *Shandong Provincial Key Laboratory of Preparation and Measurement of Building Materials, University of Jinan, Jinan 250022, China.*

[c] *Cancer Research Center, Shandong Tumor Hospital, Jinan 250012, P.R. China*

*Corresponding author: Mei Yan

E-mail: chm_yanm@126.com

Telephone: +86-531-82767161

Preparation of porous ZnO spheres and CdS NRs

The porous ZnO spheres were prepared according to the as reported literature.[1] Typically, 5 g of soluble starch was dissolved in 150 mL of boiling ultrapure water. Then, 0.01 mol of $Zn(NO_3)_2 \cdot 6H_2O$ was added and the mixture was stirred at 85 °C for 5 min. After adjusting the pH of the mixture solution to 8-9 with ammonium hydroxide, the solution was stirred for an additional 30 min at 85 °C. Subsequently, the resulting precipitate was centrifuged, washed with ultrapure water, and dried at 50 °C. Then, the as-obtained powders were calcined in air atmosphere at 500 °C for 2 h to obtain porous ZnO spheres.

The CdS NRs were synthesized via a facile solvent hydrothermal process. In a typical procedure, 1 mM cadmium chloride and 3 mM L-cysteine were dissolved into 4 mL of water to form a homogeneous solution by constant vigorous stirring. Then, 30 mL of ethylenediamine was added into the above mixture and continually stirred for 30 min. The resulting mixture was transferred into a Teflon-lined stainless-steel autoclave and heated at 180 °C for 24 h. The system was then allowed to cool to room temperature and the precipitation was collected and washed with water and absolute alcohol several times, CdS NRs were obtained and then dried under vacuum for further use.

Structure characterization

As shown in Fig. S1A, a continuous and dense conducting AuNPs layer with interconnected AuNPs was obtained completely on the cellulose fiber surfaces. The diameters of the as-synthesized ZnO spheres were about 300-500 nm (Fig. S1B). The TEM image of ZnO was shown in Fig. S1C, the prepared ZnO spheres were with rough surface. Obvious pores could be seen in ZnO, and this porous structure improved the immobilized amount of PSA. With the aid of PATP molecules, ZnO

spheres were attached onto Au-PWE (Fig. S1D) and the corresponding EDS spectrum was shown in Fig. S1E, which indicated that the ZnO was successfully immobilized on Au-PWE.

The XRD patterns of bare PWE, Au-PWE, ZnO/Au-PWE and porous ZnO spheres were shown in Fig. S1F. In contrast to the XRD pattern of bare PWE, three distinct diffraction peaks were observed in the XRD pattern of Au-PWE. The peaks at 2θ = 38.36, 44.54 and 64.75° were indexed to the (111), (200) and (220) crystallographic planes of cubic AuNPs, respectively (JCPDS card No 004-0784), suggesting that AuNPs had been successfully deposited on paper. The diffraction peaks in the range of $20° < 2\theta < 70°$ could be indexed as (100), (002), (101), (102), (110), (103), (200), (112), (201) planes of hexagonal phase ZnO, which were consistent with the value in the standard card (JCPDS 89-7102). The XRD pattern of ZnO/Au-PWE contained the diffraction peaks of Au-PWE and porous ZnO spheres, indicating that the ZnO/Au-PWE was successfully synthesized.

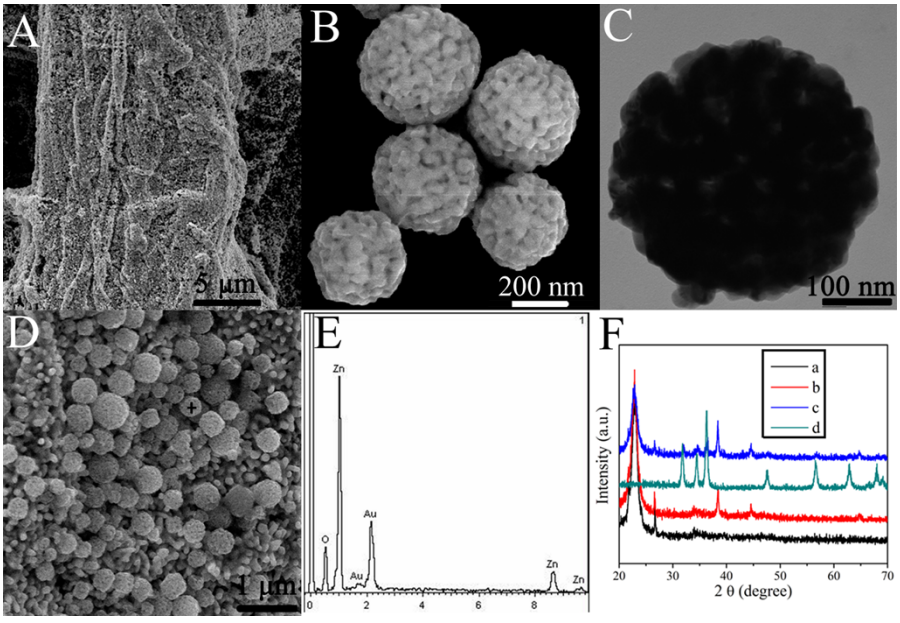

Fig. S1. SEM images of (A) Au-PWE and (B) porous ZnO spheres. (C) TEM image of ZnO. (D) SEM image of ZnO/Au-PWE. (E) EDS of ZnO/Au-PEW. (F) XRD patterns of the (a) bare paper, (b) Au-PWE, (c) ZnO/Au-PWE, (d) porous ZnO spheres.

The structure of the synthesized CdS NRs could be verified by morphological analyses. The SEM image of the CdS NRs was shown in Fig. S2A and the rod-like nanostructures of CdS with lengths about of 200 nm. The corresponding EDS spectrum of the CdS NRs was observed in Fig. S2B, the S/Cd atomic ratio was 0.94:1.0, in agreement with the stoichiometric composition of CdS. The CdS NRs-Ab-HRP bioconjugates were characterized using UV-vis spectroscopy (Fig. S2C). A broad absorption peak in visible light region was observed for the synthesized CdS NRs (curve a). After the immobilization of HRP-Ab, one adsorption peak from CdS NRs was observed at around 488 nm, and another distinct adsorption peak from the HRP-Ab was observed on the spectra of CdS NRs-Ab-HRP bio-conjugates (curve b), which was attributed to the adsorption peak from the HRP-Ab itself at 280 nm (curve c).

The XRD pattern of the as-synthesized CdS NRs was shown in Fig. S2D. The XRD pattern of CdS NRs could be ascribed to the stable hexagonal phase CdS (JCPDS No. 41-1049). The peaks at 2θ values of 24.86, 26.6, 28.24, 36.68, 43.8, 48.1, 50.9, 51.9, 52.9, 66.9 and 69.5° for CdS NRs were indexed to the (100), (002), (101), (102), (110), (103), (200), (112), (201), (203) and (210) crystal planes of wurtzite structure CdS with a hexagonal phase, respectively. No peaks of impurities were detected, revealing the high purity of the as-synthesized products. The FT-IR spectra of CdS NRs was shown in Fig. S2E, a strong absorption peak was observed at 3434 cm^{-1}, which could be attributed to the characteristic stretching vibration of $-NH_2$ group. Thus, HRP-Ab could connect to CdS NRs with the aid of GA cross-linking. The characteristic band at 1635 cm^{-1} was assigned to the flexural vibration of N-H. The peak at 581 cm^{-1} was attributed to the Cd-S stretching mode.[2]

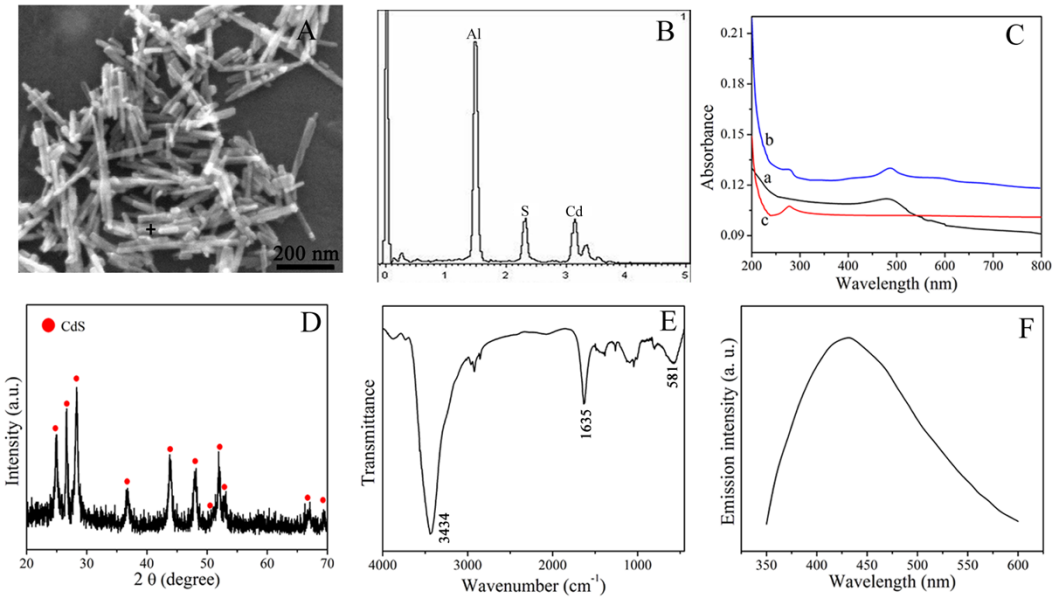

Fig. S2. (A) SEM image of CdS NRs. (B) EDS of the CdS NRs. (C) UV-vis absorption spectrum of (a) CdS NRs, (b) CdS NRs-Ab-HRP, (c) HRP-Ab. (D) XRD patterns of CdS NRs. (E) FT-IR spectra of CdS NRs. (F) CL spectrum of luminol-H_2O_2-HRP-PIP system.

Optimization of experimental conditions

A series of experiments were conducted to select optimal analytical conditions using 1 ng mL^{-1} PSA. H_2O_2 was not only used as the oxidant in the luminol-H_2O_2-HRP-PIP CL system, but also as the electron donors to suppress the corrosion of CdS under illumination as well as to facilitate the generation of stable photocurrent. At lower H_2O_2 concentration the photocurrent responses were improved with the increase of H_2O_2 concentration (Fig. S3A). When the concentration of the H_2O_2 solution was higher than 5 mM, the photocurrent intensity decreased since the oxidation of the CdS by excess H_2O_2 that yielded surface defects and traps. Thus, 5 mM H_2O_2 was used in the experiments.

As shown in Fig. S3B, the photocurrent responses increased with increasing temperature up to 37 °C, which was attributed to the increasing immunoreaction rate between PSA and CdS NRs-Ab-HRP bioconjugate. However, when temperature was over 37 °C, the photocurrent response decreased. This was attributed to high

temperature caused an irreversible denaturation of proteins. Consequently, 37 °C was employed as the optimal incubation temperature for the PEC biosensing.

Fig. S3C showed the incubation time on the responses of the PEC biosensor. At the optimized incubation temperature, the photocurrent responses increased with incubation time and reached a plateau at 25 min. Longer incubation time did not obviously improve the response, forecasting the equilibrium of immune reaction. Therefore, 25 min was accepted as the optimal incubation time.

The applied potential was an important parameter for producing the photocurrent. As shown in Fig. S3D, in the potential range from 0 to 0.4 V, the photocurrent increased slowly and trended a relatively stable value. However, the photocurrent at 0 V was 85.2% of that at +0.4 V, showing enough sensitivity for PEC detection of PSA. Meanwhile, the low applied potential was beneficial to the elimination of interference from other reductive species that coexisted in the real samples. Thus, 0 V was selected as the applied potential for the determination of PSA.

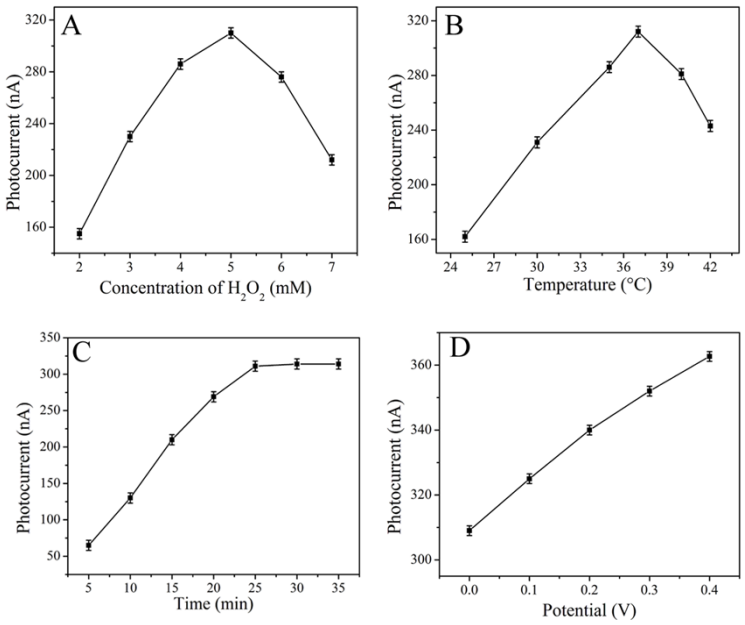

Fig. S3. The effect of (A) concentration of H_2O_2; (B) incubation temperature; (C) incubation time and (D) potential on photocurrent with 1 ng mL^{-1} PSA.

References

1 G. K. Zhang, X. Shen and Y. Q. Yang, *J. Phys. Chem. C*, 2011, **115**, 7145-7152.

2 G. Geindy, M. Mohamed and A. Mohamed, *Turk. J. Chem.*, 2006, **30**, 361-382.